Int. J. Electrochem. Sci., 16 **(2021)** Article ID: 210751, doi: 10.20964/2021.07.36

International Journal of
ELECTROCHEMICAL
SCIENCE
www.electrochemsci.org

Short Communication

Single-layer Pb^{2+} Potentiometric sensor with MoS_2 Nanoflakes as Ion-to-electron transducer

Lan Ju[1,*] *Tao Wu*[2] *Meng-xia Xu*[2] *Nan Zhang*[1]

[1] Zhejiang Fashion Institute of Technology, Ningbo 315200, P. R. China
[2] The University of Nottingham Ningbo China, Ningbo 315100, P.R. China
[*]E-mail: zjjulan@163.com

Received: 3 July 2020 / *Accepted:* 28 January 2021 / *Published:* 31 May 2021

There is a growing interest in research on all-solid-state ion-selective-electrodes (ASS-ISEs), largely motivated by simplicity, fast analytical time, and low detection limit. In this paper we report on the construction, characterization and analytical application of an ASS-ISE made using MoS_2 nanoflakes as ion-to-electron transducer. Ion-selective membrane components and MoS_2 nanoflakes were dissolved together and formed single-layer electrode. The results demonstrate that the proposed electrode has a Nernstian response slope of 27 mV/decade over a wide concentration range of 1.0×10^{-3} to 5.1×10^{-8} mol/L, and a quick response time of shorter than 5 s. The selectivity and stability are sufficient for practical application, and an example of sample measurements is given.

Keywords: Ion-selective electrodes; All solid state; Single layer; MoS_2 nanoflakes

1. INTRODUCTION

Ion-selective electrodes (ISEs) based on poly(vinyl chloride) or poly(methyl methacrylate) have attracted a great deal of attention because of their potential use in real-time analysis, due to simplicity and rapid sensing [1-5]. For applications of ISEs, it is important that electrodes possess low detection limit and stable potential signal in a wide range of ion concentration. Several approaches, including design of electrode structures and functional materials, have been used to realize the above goals [5, 6]. It has been shown that polymer ion-selective electrodes made with all-solid-state configuration exhibit a relatively improved detection limit over those using conventional inner solution [7-10]. The improvement has been attributed to the ability of the intermediate layers to make rapid ion-to-electron transduction and to reduce zero-current transmembrane ion flux effects [11, 12]. Materials proposed to

make intermediate solid contacts include redox-active self-assembled monolayer (SAM) [13, 14], carbon nanoparticles [15-19], and conducting polymers [20-25].

Nanomaterials have been widely used in a variety of fields for their unique structural and semiconductor properties [26, 27]. In the case of ISEs, it is hoped that the nanophase will modify the overall transport properties of the polymeric matrix and enhance the adhesion onto the substrate. Several groups have reported the introduction of nanomaterials to improve the electrode stability and performance. However, an aqueous layer across the electrode is observed in many cases and results in irreproducibility and long-term stability [28-30].

Molybdenum disulphide (MoS2) has been widely used as supercapacitors [31], transistors [32] and catalysts [33]. In this paper we report on single-layer ISEs fabricated by dip coating with glassy carbon substrate. They are prepared by dispersing MoS2 nanoflakes, lead ionophore and plasticizer of small molecules, into PVC matrix. The potential response as well as electrochemical impedance spectroscopy was characterized, highlighting the advantages of the single-layer structures in all-solid-state ISEs fabrication.

2. EXPERIMENTAL

2.1. Apparatus and reagents

Potassium tetrakis [3, 5-bis (trifluoromethyl)phenyl]borate (KTFPB), o-nitrophenyl octyl ether (NPOE), high molecular weight poly (vinyl chloride) (PVC), tetrahydrofuran (THF), and lead ionophore (tert-Butylcalix[4]arene-tetrakis(N,N-dimethylthioacetamide) were purchased from Sigma-Aldrich and were used as received. All solutions were prepared from analytical grade reagents and standardized as necessary. Water was distilled by a Pall Cascada laboratory water system and the specific resistance was 18.2 Mcm.

2.2. Construction of the Pb^{2+}-Selective membrane and electrodes

The membrane contains 58.3 mg of PVC (62.55 wt %), 30 mg of NPOE (32.19 wt %), 1 mg of KTFPB (1.07 wt %), 0.9 mg of lead ionophore (0.97 wt %), and 3 mg of MoS_2 nanoflakes (3.22 wt %). The mixture was dissolved in 2.0 ml of THF. The solution was then drop-casted onto the glassy carbon substrate electrodes surrounded by the PVC tubing, and dried for 2 h at room temperature. Before drop-cast, glassy carbon substrate electrodes were ultrasonically cleaned, followed by rinsing with deionized water, and acetone. The fabricated electrodes were conditioned in 1.0×10^{-4} mol/L $Pb(NO_3)_2$ before use.

2.3. Potentiometric measurements

A digital ion analyzer (Shanghai Leici Instruments Factory, China) used for measuring the potential. The emf observations were made relative to the double junction Hg/Hg_2Cl_2 electrode. All emf measurements were performed in magnetically stirred solution at room temperature in the galvanic cell. $Pb(NO_3)_2$ solutions were made by gradual dilution of 0.1 mol/L $Pb(NO_3)_2$ solution, and then the

potentiometric measurements were measured in the range 1.0×10^{-3} to 1.0×10^{-9} mol/L. All $Pb(NO_3)_2$ sample solutions had the same background of 10^{-3} mol/L $NaNO_3$.

Activity coefficients were calculated according to the Debye–Hückel procedure using the following equation:

$$\log\gamma = -0.511z^2\left[\frac{\mu^{1/2}}{1+1.5\mu^{1/2}} - 0.2\mu\right]$$

where μ is the ionic strength and z is the valency. Electromotive force (EMF) values were corrected for liquid-junction potentials with the Henderson equation.

3. RESULTS AND DISCUSSION

3.1. Potentiometric Response Characteristics

In order to achieve low limit of detection and high reproducibility, the fabricated electrodes were conditioned in in 10^{-4} mol/L $Pb(NO_3)_2$ overnight and then in 10^{-8} mol/L $Pb(NO_3)_2$ solution for 48 hours. The potentiometric response of the electrodes at varying Pb^{2+} concentrations (1.0×10^{-3} to 1.0×10^{-9} mol/L) is illustrated in Fig. 1. The detection limits were determined according to IUPAC recommendations. The detection limit calculated as the intersection of the two slope lines was 5.1×10−8 mol/L. The electrode presents a linear range between 1.0×10^{-3} and 5.1×10^{-8} mol/L for Pb^{2+} activity, and has nearly Nernstian slope of 27 mV per decade (r^2=0.996).

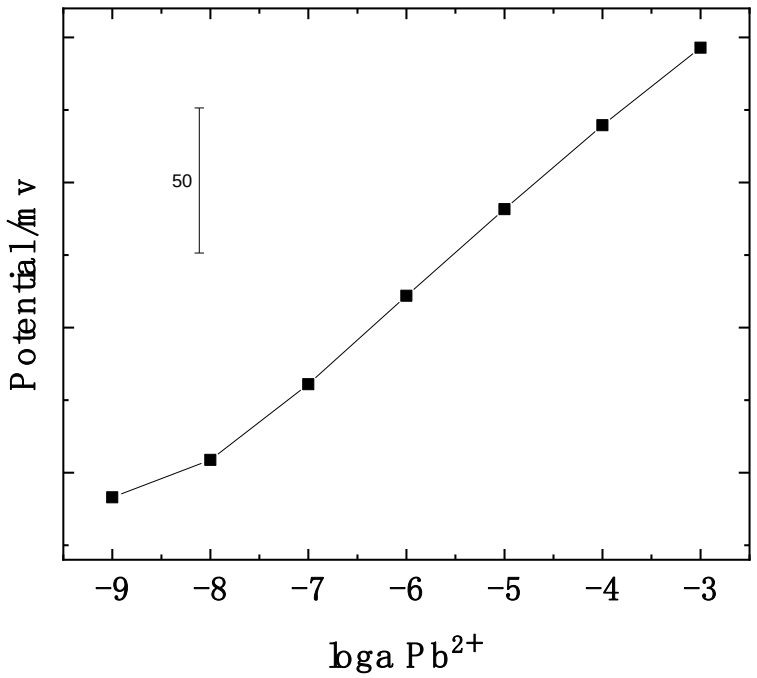

Figure 1. Potentiometric response of the single-layer Pb^{2+}-ISE electrode prepared with 3.22 wt % MoS_2 nanoflakes measured in 1.0×10^{-3} to 1.0×10^{-9} mol/L $Pb(NO_3)_2$..

Table 1 gives a comparison of linear range and slope between the proposed sensors and other Pb^{2+} potentiometric sensors that were described in literature. It has been well documented that the characteristics of the electrodes was biased by the zero-current transmembrane ion flux, and the lower detection limit is determined by transmembrane ion flux of primary ions into its aqueous surface layer [34, 35]. As a consequence, the past decade has seen dramatically improvement in ISEs behaviors in terms of detection limit, mainly due to the reduction of this flux [36-38]. In the work, we believed that ion adsorption onto MoS_2 nanoflakes was responsible for the reduction of transmembrane ion flux, therefore an lower detection limit to 5.1×10^{-8} mol/L was achieved. However, further investigation would then be carried out in order to explain this improvement.

Table 1. Linear range and slope for various lead ion-selective electrodes.

Linear range mol/L	Slope mV/decade	Reference
5×10^{-6}~1×10^{-2}	29	[3]
5×10^{-5}~5×10^{-1}	28	[8]
$10^{-5.3}$~10^{-3}	31	[9]
10^{-5}~10^{-1}	30	[18]
$1\times1^{0.6}$~1×10^{-1}	30	[22]
1×10^{-6}~1×10^{-1}	29	[26]
10^{-5}~10^{-2}	29	[28]
10^{-9}~10^{-3}	19	[37]
$10^{-9.1}$~10^{-3}	29	[38]
1×10^{-3}~5×10^{-8}	27	This work

The response time of the fabricated electrodes were measured as the length of time in which the potential variation smaller than 0.5 mV/min, after successive10-fold decrease in Pb^{2+} concentration. As can be observed from Fig. 2, the response time of the electrodes is less than 5 s for the concentrations between 1.0×10^{-3} and 5.1×10^{-8} mol/L.

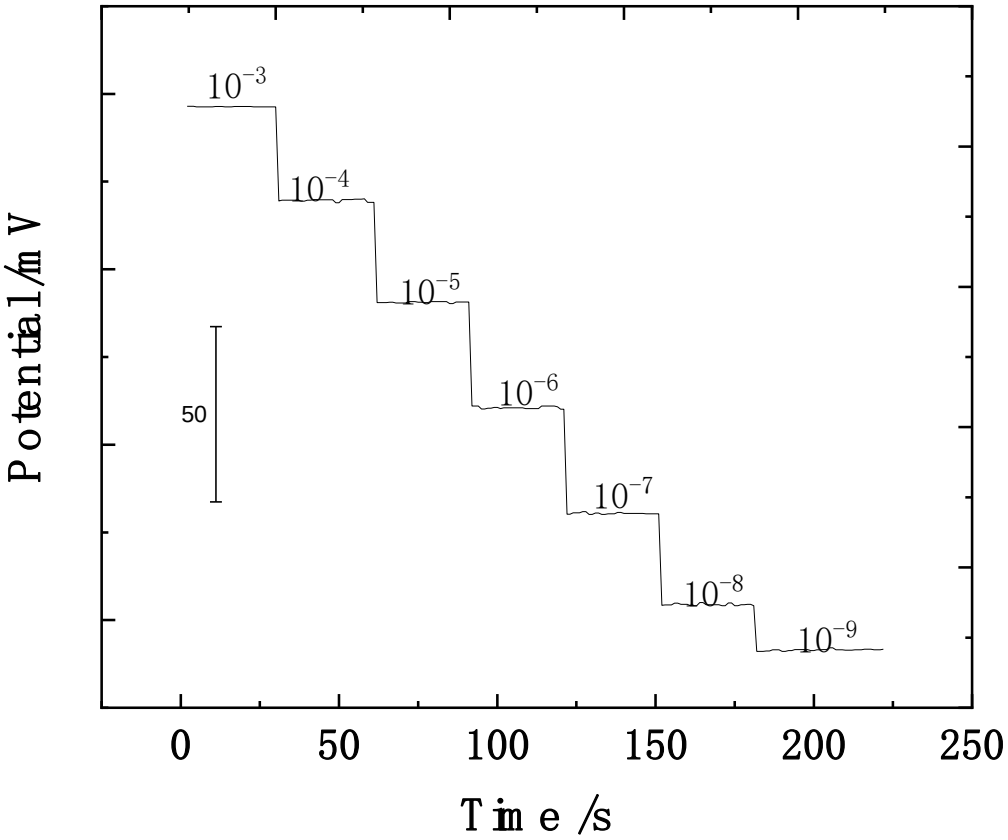

Figure 2. Time traces of potentiometric response of the single-layer Pb^{2+}-ISE electrode.

3.2. Potentiometric Selectivity

The influence of interfering ions on the potentiometric response of ion-selective electrode was characterized in terms of selectivity coefficient. Selectivity of the ion-selective electrode are quantitatively related to equilibria at the interface between the electrode membrane and the sample. In our work, the unbiased selectivity coefficients values of the electrodes in the presence of a fixed concentration of the interfering ions were evaluated by using the Bakker's separate solution method after the electrodes were conditioned in 1×10^{-3} mol/L $NaNO_3$ for 12 h. The selectivity data are illustrated in Table 2. These results showed the fabricated single-layer Pb^{2+}-ISE based on nano_ transducer give good log $K^{pot}_{Pb,J}$ than the examined interfering ions.

Table 2. Selectivity coefficients, $\log K^{pot}_{Pb,J}$, obtained with the proposed single-layer electrode based on MoS_2 nanoflakes ion-to-electron transducer.

Ion *J*	Pb^{2+}-ISE
Na^+	-6.2
K^+	-5.6
Li^+	-4.9
NH_4^+	-5.2
Ca^{2+}	-8.7
Mg^{2+}	-9.3
Zn^{2+}	-5.7
Cu^{2+}	-4.0
Cd^{2+}	-5.1

3.3. Effect of pH

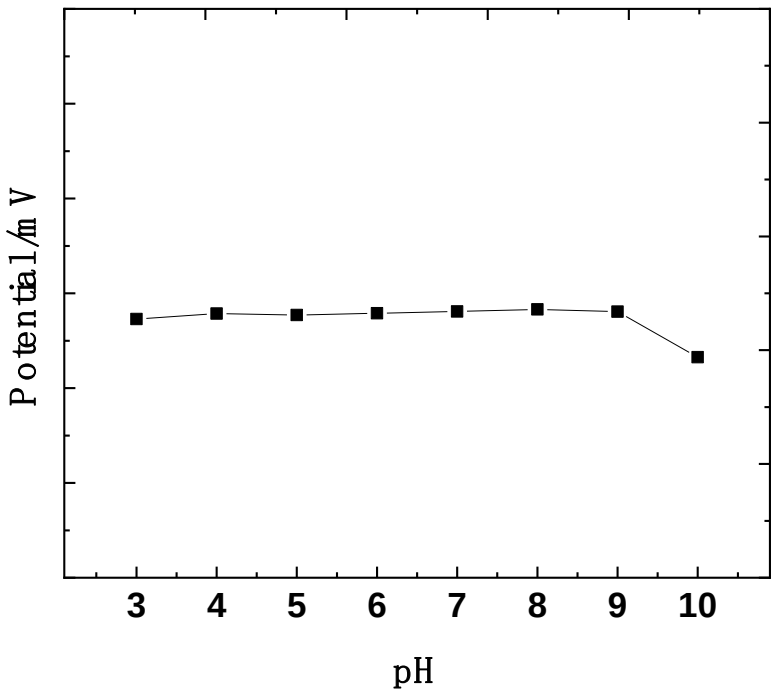

Figure 3. Effect of pH on the potential responses of the electrodes

The pH dependence of the proposed single-layer ISEs has been tested in 1×10^{-5} mol/L of lead solutions adjusted with nitric acid and ammonia. Fig. 3 indicates that the electrode is not pH sensitive in the range of pH 3.0 to 9.0, which implies that the proposed electrodes can be used in a wide range of environmental water samples without pH adjustments.

From the above results, it can be concluded that the electrode functions as well as that reported by other authors. However, there is a significant simplification of the fabrication procedure proposed in this work.

3.4. Analytical application

The above characterization makes the fabricated single-layer Pb^{2+} electrodes practically useful. In this regard, the proposed electrodes were used to monitor the concentration of Pb^{2+} in real samples.

Table 3. Potentiometric determination of Pb^{2+} using the single-layer electrode.

Samples	Pb^{2+}-ISE /10^{-7} mol/L	AAS /10^{-7} mol/L
1	1.22±0.05	1.29±0.02
2	1.96±0.05	2.21±0.03
3	3.18±0.06	3.25±0.02

Real samples were taken from Ningbo Wanda Chemical Factory. The experiment was carried out by direct potentiometry using standard addition method. The results obtained are presented in Table 3, and were compared with those obtained by atomic absorption spectrometry (AAS) method. The data demonstrates that the proposed electrodes can be successfully used to determine Pb^{2+} in real samples.

4. CONCLUSION

A single-layer Pb^{2+} ISE was prepared by using MoS_2 nanoflakes for the first time as ion-to-electron transducer. The proposed electrode exhibit a wide linear range (1×10^{-3} to 5.1×10^{-8} mol/L) with respect to Pb^{2+} concentration with good Nernstian slope (27 mVdecade^{-1}). The response time was shorter than 5 s and the electrode showed good selectivity over common alkali, alkaline earth and heavy metal ions. The potentiometric drifts were less than 10% for one month and was independent of pH in the range of 3.0 and 9.0. The results revealed that the single-layer ISE can be used successfully to determine Pb^{2+} contents in real samples.

ACKNOWLEDGEMENTS
This work was financially supported by the Ningbo Natural Science Foundation(No.2010A610151), the Xinmiao Talents Project of Zhejiang province(No.2017R475003).

CONFLICTS OF INTEREST
There are no conflicts to declare.

References

1. M. Novell, M. Parrilla, G. A. Crespo, F. X. Rius, F. J. Andrade, *Anal. Chem*., 84 (2012) 4695-4702.
2. S. Y. Yu, L. Ju, T. Xiong, Y. C. Li, Y. M. Liu, *Int. J. Electrochem. Sci*., 10 (2015) 6684-6689.
3. H. R. Pouretedal, M. H. Keshavarz, *Asian J. Chem*., 16 (2004) 1319-1326.
4. Y. Kang, K. Gwon, J. H. Shin, H. Nam, M. E. Meyerhoff, G. S. Cha, *Anal. Chem*., 83 (2011) 3957-3962.
5. A. Rzewuska, M. Wojciechowski, E. Bulska, E. A. H. Hall, K. Maksymiuk, A. Michalska, *Anal. Chem.* 80 (2008) 321-327.
6. M. A. Fierke, C. Z. Lai, P. Buhlmann, A. Stein, *Anal. Chem*., 82 (2010) 680-688.
7. R. Zielinska, E. Mulik, A. Michalska, S. Achmatowicz, M. Maj-Zurawska, *Anal. Chim. Acta*, 451 (2002) 243-249.
8. C. C. Su, M. C. Chang, L. K. Liu, *Anal. Chim. Acta*, 432 (2001) 261-267.
9. X. H. Yang, N. Kumar, D. B. Hibbert, *Electroanalysis*, 10 (1998) 827-831.
10. M. Gutierrez, V. M. Moo, S. Alegret, L. Leija, P. R. Hernandez, R. Munoz, M. del Valle, *Microchim. Acta*, 163 (2008) 81-88.
11. S. Y. Yu, and Q. Yuan, *Talanta*, 24 (2012) 2021-2025.
12. C. Dumschat, M. Borchardt, C. Diekmann, K. Cammann, and M. Knoll, *Sens. Actuat. B: Chem*., 24 (1995) 279-281.
13. M. Fibbioli, K. Bandyopadhyay, S. G. Liu, L. Echegoyen, O. Enger, F. Diederich, D. Gingery, P. Buhlmann, H. Persson, U. Suter, E. Pretsch, *Chem. Mater*., 14 (2002) 1721-1729.
14. S. Gracheva, C. Livingstone, J. Davis, *Anal. Chem*., 76 (2004) 3833-3836.
15. T. Lindfors, H. Aarnio, A. Ivaska, *Anal. Chem*., 79 (2007) 8571-8577.
16. F. H. Li, J. J. Ye, M. Zhou, S. Y. Gan, Q. X. Zhang, D. X. Han, L. Niu, *Analyst*, 137 (2012) 618-623.
17. J. B. Hu, X. U. Zou, A. Stein, P. Bühlmann, *Anal. Chem*., 86 (2014) 7111-7118.
18. M.K. Amini, M. Mazloum, A. A. Ensafi, *J. Anal. Chem*., 364 (1999) 690-693.
19. B. Paczosa Bator, L. Cabaj, R. Piech, K. Skupien, *Analyst*, 137 (2012) 5272-5277.
20. S. Y. Yu, F. H. Li, *Anal. Chim. Acta*, 702 (2011) 195-198.
21. S. H. Xu, Q. Yuan, S. Y. Yu, *Electroanalysis*, 101 (2012) 546-549.
22. V.S. Bhat,V.S. Ijeri, A.K. Srivastava, *Sens. Actuators B: Chem*., 99 (2004) 98-105.
23. S. Y. Yu, L. Ju, T. Xiong, Y. C. Li, Y. M. Liu, *Int. J. Electrochem. Sci*., 10 (2015) 5994-6001.
24. S. Y. Yu, F. H. Li, *Sens. Actuat. B: Chem*., 155 (2011) 919-922.
25. S. Y. Yu, Y. C. Li, T. Xiong, *Chinese Chem. Lett*., 25 (2014) 364-366.
26. L. X. Chen, J. Zhang, W. F. Zhao, *J. Electroanal. Chem*., 589 (2006) 106-111.
27. M. Acerce, D. Voiry, M. Chhowalla, *Nat. Nanotechnol*., 10 (2015) 313-318.
28. F. Cadogan, P. Kane, M. A. McKervey, *Anal. Chem*., 71 (1999) 5544-5550.
29. M. Fibbioli, W. E. Morf, M. Badertscher, N. F. de Rooij, E. Pretsch, *Electroanalysis*, 12 (2000) 1286-1292.
30. G. D. O'Neil, R. Buiculescu, S. P. Kounaves, N. A. Chaniotakis, *Anal. Chem*., 83 (2011) 5749-5753.
31. B. Radisavljevic, A. Radenovic, J. Brivio, V. Giacometti, A. Kis, *Nat. Nanotechnol*., 6 (2011) 147-

150.
32. Z. Y. Wang, H. Li, Z. Liu, Z. J. Shi, J. Lu, K. Suenaga, S. K. Joung, T. Okazaki, Z. N. Gu, J. Zhou, Z. X. Gao, G. P. Li, S. Sanvito, E. G. Wang, S. Iijima, *J. Am. Chem. Soc*., 132 (2010) 13840-13847.
33. A. N. Dhas, K. S. Suslick, *J. Am. Chem. Soc*., 71 (2005) 2368-2369.
34. T. Sokalsk, T. Zwickl, E. Bakker, E. Pretsch, *Anal. Chem*., 71 (1999) 1204-1209.
35. T. Sokalski, A. Ceresa, M. Fibbioli, T. Zwickl, E. Bakker, E. Pretsch*, Anal. Chem*., 71 (1999) 1210-1214.
36. I. Bedlechowicz-Śliwakowska, P. Lingenfelter, T. Sokalski, A. Lewenstam, M. Maj-Żurawska, *Anal. Bioanal. Chem.* 385 (2006) 1477-1482.
37. J. Sutter, E. Lindner, R. E. Gyurcsanyi, E. Pretsch, *Anal. Bioanal. Chem*., 380 (2004) 7-14.
38. X. H. Zeng, W. E. Jiang, X. H. Jiang, G. I. N. Waterhouse, Z. M. Zhang, L. M. Yu, *Anal. Chim. Acta,* 1094 (2020) 26-33.